Influence of the Attaching Group and Substituted Position in the Photosensitization Behavior of Ruthenium Polypyridyl Complexes

Yuan-jun Hou, Pu-hui Xie, Bao-wen Zhang,* Yi Cao,* Xu-rui Xiao, and Wei-bo Wang

Institute of Photographic Chemistry, Chinese Academy of Sciences, Beijing 100101, China

Received January 5, 1999

Introduction

There has been intense research in the sensitization of large band gap semiconductor oxides since the breakthrough of the photoelectrochemical solar cell was accomplished by Gratzel and co-workers. The light-to-electrical conversion efficiency of the solar cell was up to 10%.[1] For the efficient sensitizers used in the solar cells, the main requirements are as follows: (i) broad absorption spectra, (ii) suitable ground- and excited-state photoelectrochemical properties, and (iii) high stability in the oxidized state.[2] Ruthenium polypyridyl complexes have proven to currently be the most efficient.

Despite a considerable and widespread research interest, a comprehensive fundamental understanding of the structure−function relationship is lacking. In this paper we report on the preparation and spectroscopic and photoelectrochemical properties of *cis*-$(NCS)_2$-bis(2,2′-bipyridyl-3,3′-dicarboxylic acid)-ruthenium(II), *cis*-$(NCS)_2$-bis(2,2′-bipyridyl-5,5′-dicarboxylic acid)ruthenium(II), and Ru(II) complexes having the general formula *cis*-$(NCS)_2$-bis(4,4′-disubstituted-2,2′-bipyridine)ruthenium(II), where the substituent is CO_2Et, CH_2OH, or COOH. The compounds designed and synthesized allow us to study the influence of the attaching group on their photoelectrochemical properties. In addition, the results of the photosensitization behavior of the ruthenium complexes with carboxyl groups at different positions of 2,2′-bipyridine are also given in this paper.

Experimental Section

Materials. *N*,*N*-Dimethylformamide (DMF) was purified by distillation under reduced pressure after being dried with $MgSO_4$ for 24 h, and all the other solvents and chemicals were used as purchased. 2,2′-Bipyridine-3,3′-dicarboxylic acid (abbreviated [3,3′-(LL)]),[3] 2,2′-bipydine-4,4′-dicarboxylic acid (abbreviated [4,4′-(LL)]),[4] 4,4′-diethylcarboxylate-2,2′-bipyridine (abbreviated [bpy-CO_2Et]),[4] 2,2′-bipyridine-5,5′-dicarboxylic acid (abbreviated [5,5′-(LL)]),[5] and 4-(hydroxymethyl)-4′-methyl-2,2′-bipyridine (abbreviated [bpy-CH_2OH])[6] were prepared according to literature procedures. *cis*-[3,3′-(LL)]$_2$Ru(Cl)$_2$, *cis*-[4,4′-(LL)]$_2$Ru(Cl)$_2$, and *cis*-[4,4′-(LL)]$_2$Ru(NCS)$_2$ **(II)** were prepared by the method described by Gratzel et al.[2] *cis*-[5,5′-(LL)]$_2$Ru(Cl)$_2$ and *cis*-[5,5′-(LL)]$_2$Ru(NCS)$_2$ **(III)** were synthesized by the method in the literature.[7]

Preparations. *cis*-Ru[bpy-CO_2Et]$_2$(Cl)$_2$. A 121.6 mg sample of $RuCl_3\cdot 3H_2O$ (Aldrich) and 279.8 mg of ligand [bpy-CO_2Et] were dissolved in 80 mL of ethanol and refluxed under argon for 3 days. The solution was concentrated under vacuum. After cooling, the complex was precipitated by addition of ether. The violet red product was recrystallized from methanol−acetone.

***cis*-Ru[bpy-CO_2Et]$_2$(NCS)$_2$.** A 100 mg sample of *cis*-Ru[bpy-CO_2Et]$_2$(Cl)$_2$ was dissolved in 50 mL of ethanol in the dark. Sodium thiocyanate (NaSCN; 50 mg) was dissolved in 1 mL of H_2O and subsequently added to the above solution. The reaction mixture was then heated to reflux for 48 h under an argon atmosphere, while magnetic stirring was maintained. After this time, the reaction mixture was allowed to cool, and the solvent was removed on a rotary evaporator. The resulting solid was washed well with H_2O. The violet product was recrystallized with methanol−ether. Anal. Calcd for $RuC_{34}H_{32}N_6O_8S_2\cdot 3H_2O$: C, 46.83; H, 4.35; N, 9.63. Found: C, 47.03; H, 4.08; N, 9.70.

bpy-CH_2OH.[6] **(A) 4-Formyl-4′-methylbipyridine.** 4,4′-Dimethyl-2,2′-bipyridine (1 g, 0.0055 mmol) was dissolved in 200 mL of 1,4-dioxane, selenium(IV) oxide (1 g, 0.009 mmol) was added, and the solution was refluxed for 40 h. The yellow solution was filtered to remove the black precipitate, and the dioxane was removed by rotary evaporating. The solid was redissolved in chloroform, and the solution was filtered to remove excess selenium byproducts. The chloroform was then removed under reduced pressure. The chloroform suspension and filtration steps were repeated as needed to remove all of the selenium byproducts. A light yellow solid was obtained. ^{1}H NMR ($CDCl_3$): δ 2.43 (CH_3); 10.18 (CHO); 7.15−8.93 (aromatic).

(B) 4-(Hydroxymethyl)-4′-methylbipyridine. 4-Formyl-4′-methylbipyridine (3.8 g, 0.020 mmol) was dissolved in 30 mL of methanol. Sodium borohydride (0.76 g, 0.020 mmol) in 6 mL of NaOH (0.2 M) was added dropwise to the solution cooled on ice. The reaction was allowed to continue for 1 h at room temperature. The black precipitate was removed by filtration, and the methanol was removed under reduced pressure. The remaining aqueous suspension was diluted with 10 mL of sodium carbonate solution and then extracted with chloroform. The chloroform solution was dried over magnesium sulfate, and the chloroform was removed. ^{1}H NMR ($CDCl_3$): δ 2.42 (CH_3); 4.79 (CH_2O); 7.034−8.62 (aromatic).

***cis*-Ru[bpy-CH_2OH]$_2$(Cl)$_2$.** The procedure used to prepare the *cis*-Ru[bpy-CH_2OH]$_2$(Cl)$_2$ complex is analogous to that used to prepare *cis*-Ru[bpy-CO_2Et]$_2$(Cl)$_2$ except that the reaction solvent is changed to DMF and the refluxing time is reduced to 24 h.

***cis*-Ru[bpy-CH_2OH]$_2$(NCS)$_2$.** The procedure used to prepare the *cis*-Ru[bpy-CH_2OH]$_2$(NCS)$_2$ complex is analogous to that used to prepare *cis*-Ru[bpy-CO_2Et]$_2$(NCS)$_2$ except that the reaction solvent is changed to DMF and the refluxing time is reduced to 24 h. Anal. Calcd for $RuC_{26}H_{24}N_6O_2S_2\cdot 2H_2O$: C, 47.72; H, 4.28; N, 12.85. Found: C, 47.83; H, 4.38; N, 13.13.

***cis*-Ru[3,3′-(LL)]$_2$(NCS)$_2$ (I).** A 283 mg sample of *cis*-Ru[3,3′-(LL)]$_2$(Cl)$_2$ was dissolved in 30 mL of methanol in the dark. To this solution was added 20 mL of a 0.1 M aqueous NaOH solution to deprotonate the carboxy groups. Sodium thiocyanate (NaSCN; 350 mg) was dissolved in 2 mL of H_2O and subsequently added to the above solution. The reaction mixture was then heated to reflux for 24 h under an argon atmosphere, while magnetic stirring was maintained. After this time, the reaction mixture was allowed to cool, and the solvent was removed on a rotary evaporator. The resulting solid was dissolved in H_2O and filtered through a sintered glass crucible. The pH of this filtrate was lowered to 2 by adding dilute $HClO_4$, and precipitate appeared. The violet red solid was washed with H_2O followed by

(1) Morrison, S. R. *Electrochemistry of Semiconductor and Oxidized Metal Electrodes*; Plenum Press: New York, 1980; see also references therein.
(2) Nazeeruddin, M. K.; Kay, A.; Rodicio, I.; HumphryBaker, R.; Muller, E.; Liska, P.; Viachopoulos, N.; Gratzel, M. *J. Am. Chem. Soc.* **1993**, *115*, 6382.
(3) Wimmer, F. L.; Wimmer, S. *OPPI BRIEFS* **1983**, *15* (5), 368.
(4) Case, F. H. *J. Am. Chem. Soc.* **1946**, *68*, 2574.
(5) Sprintschnik, G.; Sprintschnik, H. W.; Kirsh, P. P.; Whitten, D. G. *J. Am. Chem. Soc.* **1977**, *99*, 4947.
(6) Geren, L.; Hahm, S.; Durham, B.; Millett, F. *Biochemistry* **1991**, *30*, 9450.
(7) Argazzi, R.; Bignozzi, C. A.; Heimer, T. A.; Castellan, F. A.; Meyer, G. A. *Inorg.Chem.* **1994**, *33*, 5774.

10.1021/ic990001w CCC: $18.00
Published on Web 12/03/1999

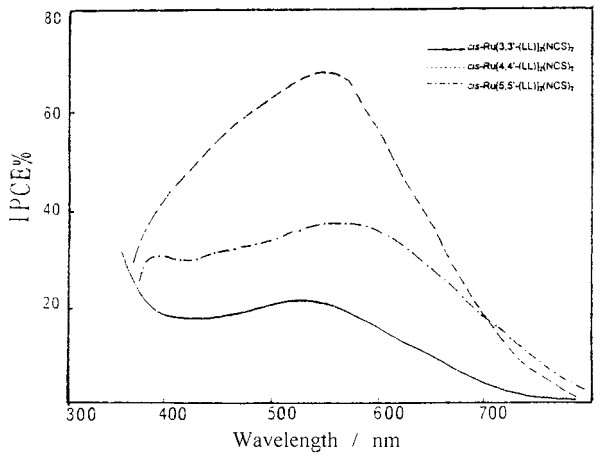

Figure 1. Photocurrent action spectra for nanocrystalline TiO_2 films coated with $RuL_2(NCS)_2$.

anhydrous diethyl ether, and air-dried for 1 h. Anal. Calcd for $RuC_{26}H_{16}N_6O_8S_2 \cdot 4H_2O$: C, 40.16; H, 3.08; N, 10.80. Found: C, 39.75; H, 2.54; N, 10.83.

Preparation of Nanocrystalline TiO_2 Films. The TiO_2 electrodes were prepared using a published technique.[2] A 12 g sample of the commercial TiO_2 powder (P25, Degussa AG, Germany, a mixture of ca. 30% rutile and 70% anatase, mean size of primary particles about 25 nm) was ground in a porcelain mortar with a small amount of water (4 mL) containing acetylacetone (0.4 mL) to prevent reaggregation of the particles. After the powder had been dispersed by the high shear forces in the viscous paste, it was diluted by slow addition of water (16 mL) under continued grinding. Finally, a detergent (0.2 mL of Triton X-100, Aldich) was added. This viscous dispersion of colloidal TiO_2 particles was spread on a fluorine-doped SnO_2 conducting glass support (resistance 20 Ω/cm^2). After air drying, the electrode was fired for 30 min at 450−550 °C in air.

Coating of the TiO_2 surface with dye was carried out by soaking the film for 8 h in a 3×10^{-4} M solution of the ruthenium complex in dry ethanol. The electrode was dipped into the dye solution while it was still hot, i.e., while its temperature was ca. 80 °C.

The amount of adsorbed dye was determined by desorbing the dye from the TiO_2 surface into a solution of 10^{-4} M NaOH in ethanol and measuring its absorption spectrum. Surface coverages were independently verified by spectroscopic measurement of the amount of complex in the ethanol solution before and after the attachment process.

Photoelectrochemistry. Photoelectrochemical experiments employed the dye-sensitized TiO_2 film incorporated into a thin-layer sandwich-type solar cell. The counter electrode was prepared by sputtering a thin layer of platinum onto the conductive side of a tin oxide electrode similar in size to the working electrode. The electrolyte was 0.5 M KI and 0.05 M I_2 in propylene carbonate/ethylene carbonate (v/v, 2:8) sandwiched between the Pt and TiO_2 electrodes. The Pt electrode and the dye-coated TiO_2 electrode were clamped firmly together, and a small quantity of redox electrolyte solution was introduced into the porous structure of the TiO_2 film by capillary action.

Results and Discussion

1. Effect of Carboxyl Group Substituting Position. Figure 1 displays the photocurrent action spectra obtained with the nanocrystalline TiO_2 films coated with a monolayer of 3,3′-, 4,4′-, and 5,5′-based dyes. The incident monochromatic photon-to-current conversion efficiency (IPCE), defined as the number of electrons generated by light in the external circuit divided by the number of incident photons, is a key parameter of cell performance. It can be obtained from the photocurrents by means of the following equation:

$$\mathrm{IPCE}(\lambda) = \frac{(1.24 \times 10^3\ \mathrm{eV.nm}) \times \mathrm{photocurrentdensity}\ (\mu\mathrm{A/cm^2})}{\mathrm{wavelength\ (nm)} \times \mathrm{photonflux}\ (\mu\mathrm{W/cm^2})} \quad (1)$$

The photocurrent action spectrum is a plot of IPCE versus excitation wavelength. Relevant optical, electrochemical, and photoelectrochemical properties of the above three sensitizers are summarized in Table 1.

An examination of Figure 1 and Table 1 reveals that there is a substantial decrease in IPCE upon the substituted position of the carboxylic acid group going from 4,4′- to 3,3′- and 5,5′- of 2,2′-bipyridine. The maximum of IPCE for 4,4′-based dye is greater than 70%, while those for the 3,3′- and 5,5′-based dyes are 21% and 36%, respectively. Therefore, the substituted position has profound influence on photophysical and electrooptical properties of the ruthenium polypyridyl complexes.

To rationalize these observations and understand the factors which have an impact on IPCE more clearly, IPCE is expressed in terms of the light-harvesting efficiency (LHE), the quantum yield of charge injection (Φ_{inj}), and the efficiency of collecting the injected charge at back contact (η_c)

$$\mathrm{IPCE}(\lambda) = \Phi_{inj}(\mathrm{LHE}(\lambda))\eta_c \quad (2)$$

(1) Light-Harvesting Efficiency. LHE is given by

$$\mathrm{LHE}(\lambda) = 1 - 10^{-\Gamma\sigma(\lambda)} \quad (3)$$

where Γ is the number of moles of sensitizer per square centimeter of projected surface area of the film and σ is the absorption cross section in units of cm^2/mol obtained from the decadic extinction coefficient ($M^{-1}\ cm^{-1}$) by multiplication by 1000 cm^3/L. The data shown in Table 1 imply that, independent of the dyes, the final surface coverages on TiO_2 films (Γ) are the same within experimental error. The difference in Γ values and the lower extinction coefficients for 3,3′- and 5,5′-based dyes result in a lower LHE. However, eq 3 gives only a lower limit for the light-harvesting effeciencies because the films employed scatter light significantly, leading to enhanced absorption. Thus, LHE cannot account for the differences in IPCE.

(2) Electron Collection Efficiency. It is generally believed that for sensitizers with similar Ru(III/II) reduction potentials anchored to the same materials, the electron collection efficiency is independent of the sensitizer. The data in Table 1 support the above conclusion.

(3) Electron Injection Quantum Yield. Φ_{inj} is given by

$$\Phi_{inj} = \frac{k_{inj}}{k_r + k_{nr} + k_{inj}} \quad (4)$$

where k_r and k_{nr} are the radiative and nonradiative rate constants for the excited dye and k_{inj} is the electron injection rate. Meyer and co-workers interpreted that 5,5′-based sensitizers are less efficient at converting visible photons into electrons in terms of nonradiative decay of excited states (direct deactivation channel) competing effectively with electron injection, thereby lowering Φ_{inj} in eq 4.[7]

The experimental results reveal that the π^* level of 3,3′-based dyes is increased, which can be proven by the blue shift of λ_{max}, and the metal redox potential is roughly constant. Therefore, the energy gap of the 3,3′-based dye is larger than that of the 4,4′-based dye.

On the basis of Fermi's Golden Rule,[10] the rate of radiative decay is proportional to the product of the square of the

Table 1. Absorption and Electrochemical and Photoelectrochemical Properties of $RuL_2(NCS)_2$

complex	$\lambda_{abs\ max}$[a] (nm)	E_0[b] (V, vs SCE)	I_{sc} (mA/cm^2)	V_{oc} (V)	$10^7\Gamma$ (mol/cm^2)	LHE	max IPCE
I (3,3′)	500	0.87	8.0	0.47	1.69	0.824	0.213
II (4,4′)	535	0.85	18.4	0.57	2.10	0.951	0.71
III (5,5′)	575	0.95	7.8	0.49	2.10	0.806	0.366

[a] Measured in CH_3OH. [b] Electrolyte was tetrafluoroborate tetrabutylammonium salt/EtOH; all potentials reported vs SCE.

transition dipole moment and the cube of the radiative energy gap between the ^{3}MLCT and $^1A_1$ states (i.e., the energy of emission), eq 5. In the present case, the transition dipole moment for the excited-state to ground-state transition is slightly changed. According to eq 5, k_r of the 3,3′-based dye is larger than that of the 4,4′-based one.

$$k_r \propto \langle \vec{\mu} \rangle^2 (\bar{\nu})^3 \tag{5}$$

For the 3,3′-based sensitizer, the bite angle cannot be optimized because of the steric hindrance in the 3,3′-positions of 2,2′-bipyridine. Thus, a weakening of the ligand field is induced by steric effects.[8] The weakened ligand field leads to a decrease in the energy of the high-lying ligand field (^{3}LF) excited state of the 3,3′-based dye, making thermally activated ^{3}MLCT (metal-to-ligand charge-transfer state) to ^{3}LF internal conversion more facile.[9] Therefore, k_{nr} (indirect, thermally activated decay pathway) increases exponentially with decreasing energy gap between the MLCT and LF excited states. An increase both in k_r and in k_{nr} maybe one of the reasons that the performance of the 3,3′-based sensitizer is not as good as that of the 4,4′-based dye.

It is difficult to characterize the properties of excited states of these $Ru(bpy\text{-}X_2)(NCS)_2$ complexes because their emitting states have very low luminescence quantum yields (for 4,4′-based molecules, 0.4% at 125 K) and very short lifetimes (50 ns at 298 K for the 4,4′-based dyes).[11] Thus, the fluorescence and its lifetime of the 3,3′-based dye were undectable at room temperature. However, recent photophysical studies from our laboratory have shown unequivocally that the fluorescence lifetime and quantum yield of $[Ru(bpy)_2$(3,3′-dicarboxylic acid-2,2′-bipyridine)$]^{2+}$ are smaller than those of $[Ru(bpy)_2$(4,4′-dicarboxylic acid-2,2′-bipyridine)$]^{2+}$ (56 ns versus 176 ns in fluorescence lifetime and 3.75×10^{-3} versus 8.96×10^{-3} in quantum yield).[12] These experimental results provide evidence for our above conclusion.

2. Effect of the Attaching Group. The mode of binding turns out to be another factor that affects the electronic coupling. The influence of surface binding on the photoelectrochemical properties of sensitizers by using complexes with different attaching groups on the ligands is investigated. The results are listed in Table 2.

Table 2. Performance Characteristics of Photovoltaic Cells Based on Nanocrystalline TiO_2 Films Sensitized by $RuL_2(NCS)_2$

complex	I_{sc} (mA/cm^2)	V_{oc} (mV)	ff	η (%)
bpy-CO_2Et	1.8	380	0.47	0.5
bpy-CH_2OH	10	510	0.48	3.8
4,4′-(LL)	18	570	0.41	7.0

When the attaching group is carboxylic acid, intimate electronic coupling is observed between its excited-state wave function and the conduction band manifold of the semiconductor. However, in the case of (bpy-CO_2Et), H-bonding is the unique mode of binding on TiO_2. It is clear that the electronic coupling of the ester-type linkage is stronger than that of H-bonding. This conclusion is consistent with the performance of sensitizers on the nanocrystalline TiO_2 electrodes, but the photoelectrochemical properties of (bpy-CH_2OH) bound to the surface with H-bonding are much better than those of (bpy-CO_2Et). Possible explanations for the observation are as follows.

(1) Because the hydroxymethyl group is smaller in size and more flexible, it can bind with Ti^{4+} at different distances and angles. It can also be adsorbed on Ti^{4+} centers deeply buried below the O^{2-} ions. The electronic coupling of the hydroxymethyl group with the TiO_2 surface is stronger than that of the ester.

(2) The ligands with a electron-donating group have the effect of destabilizing the dσ*-orbital, which results in a large dπ−dσ* energy gap. Thus, the nonradiative rate constant decreases exponentially.

Conclusion

The experimental results suggest that the steric factor influences the excited-state energy level of the sensitizers. Since the rate constant for electron injection decreases and the rate of nonradiative decay increases, it can be concluded that 3,3′- and 5,5′-based sensitizers are less efficient at converting visible photons into electrons than *cis*-Ru[4,4′-(LL)]$_2(NCS)_2$.

It was also found that the attaching group could alter the interaction between the sensitizers and surfaces of TiO_2 nanocrystalline electrodes, and a good effect of sensitization can only be obtained when the interaction between the sensitizer and the surface of the nanocrystalline semiconductor is strong enough to create a stable surface structure. Therefore, light-to-electric energy conversion efficiencies of sensitizers with different attaching groups decrease in the order carboxylic acid group, hydroxy group, and ester group.

Acknowledgment. The work is supported by the NNSFC (Grants 29672034 and 29733100).

IC990001W

(8) Balzani, V.; Barigelletti, F.; Campagna, S.; Balzer, P.; von Zelewsky, A. *Coord. Chem. Rev.* **1988**, *84*, 85.
(9) Fernando, S. R. L.; Michael, Y. O. *J. Chem. Soc., Chem. Commun.* **1996**, 637.
(10) Kestner, N. R.; Jortner, J. *J. Phys. Chem.* **1974**, *78*, 2148.
(11) Ferrere, S.; Gregg, B. A. *J. Am. Chem. Soc.* **1998**, *120*, 843.
(12) Xie, P.-h.; Hou, Y.-j.; Zhang, B.-w.; Cao, Y. *J. Photochem. Photobiol., A* **1999**, *122*, 169.
(13) Meyer, T. J.; Meyer, G. J.; Pfennig, B. W.; Schoonover, J. R.; Timpson, C. J.; Wall, J. F.; Kobusch, C.; Chen, X.; Peek, B. M.; Wall, C. G.; Ou, W.; Erickson, B. W.; Bignozzi, C. A. *Inorg. Chem.* **1994**, *33*, 3952.
(14) Deacon, G. B.; Phillips, R. J. *Coord. Chem. Rev.* **1980**, *33*, 227.